Flow of Drilling Fluids Between Eccentric Rotating Cylinders

Dennis A. Siginer[1] and Sayavur Bakhtiyarov[2]

1- Department of Mechanical Engineering, Auburn University
Auburn, AL 36849, USA
2-Department of Theoretical Mechanics, Azerbaijan State Oil Academy
Baku, Azerbaijan

ABSTRACT

The effect of pipe eccentricity on the flow of well bore fluids in annuli is investigated both analytically and experimentally. The expression for azimuthal velocity as a function of the eccentricity ratio and rheological parameters of the fluid has been obtained analytically using Kutateladze-Popov-Khabakhpasheva's linear fluidity model. Velocity profiles were measured for a Newtonian glycerol/water mixture and a non-Newtonian oil field spacer fluid in eccentric annuli using the stroboscopic flow visualization method. Measured velocity profiles in the eccentric annulus compare well to analytical predictions.

INTRODUCTION

The effect of pipe eccentricity on the flow of well bore fluids in annuli is seldom taken into account in simulations used to design or evaluate drilling and cementing operations in oil fields. Nevertheless, pipe eccentricity plays a predominant role in the mud-circulation and mud-displacement processes. It is well established that pipe movement, reciprocation or rotation, or both simultaneously, during mud conditioning and cementing improves the chances for a successful drill or cementing operation. The flow of drilling fluids between eccentric tubes is an important problem relevant to drilling and cementing technology. The laminar flow of a viscous fluid bounded by a stationary outer tube and a rotating inner tube can separate at sufficiently large eccentricities resulting in a counter-rotating eddy. The existence of the eddy considerably reduces the efficiency of drilling and cementing operations. The larger is the closed circulation region the less efficient the drilling or cementing operation becomes. For instance in drilling, cuttings mixed with drilling fluids are removed through the eccentric annulus between the rotating drill pipe and the stationary outer wall. The counter-rotating eddy may reduce the removal efficiency by reducing the effective flow area and by trapping a considerable volume of cuttings. The efficiency of the cuttings transport to the surface can be substantially increased by varying the size of the resulting eddy at a given eccentricity. The size of the separated region also has an impact on the successful removal of the drilling fluid from the annulus by the cementing fluid.

Special muds and cements have been developed in oil industry to provide better drilling and annular sealing in oil wells. Most of them exhibit non-Newtonian properties. The rheological properties of a wide range of nonlinear fluids used in oil wells may be adequately described by the Kutateladze-Popov-Khabakhpasheva linear fluidity constitutive model. This paper describes the results of the analytical and experimental investigation of the flow of linear fluidity type fluids between eccentric pipes. The stroboscopic visualization technique is used to measure azimuthal velocity profiles at various angular positions and eccentricities.

THEORETICAL

The geometry of the eccentric annulus is shown in Fig. 1. The inner pipe of radius R rotates with angular velocity ω relative to a stationary outer pipe of radius R_0. e is the eccentricity.

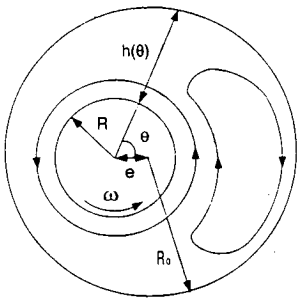

To describe the nonlinear viscosity of the fluid between eccentric cylinders, the concept of fluidity is used. Fluidity $\varphi(\tau)$ is defined as the reciprocal of the viscosity μ

$$\varphi(I_2) = [\mu(J_2)]^{-1} = \varphi_0 + \kappa(0.5|I_2|)^{0.5} ,$$

where J_2 and I_2 refer to the second invariants of the rate of deformation and stress tensors, respectively.

The velocity field can be obtained from the momentum balance,

$$\rho\frac{D\underset{\sim}{u}}{Dt} = -\nabla P + \nabla\cdot(\varphi^{-1}\underset{\sim}{D}) ,$$

under the lubrication approximation, that is, when the flow in the narrow eccentric annulus is approximated by variable gap channel flow. There is no flow due to either drag or pressure gradient in the direction of the tubes axes. (x) is the coordinate along the unfolded inner tube with (y) coordinate extending into the gap,

$$\left|\frac{\partial P}{\partial y}\right| \ll \left|\frac{\partial P}{\partial x}\right| , \quad |v| \ll |u| , \quad \underset{\sim}{u} = u\underset{\sim}{e}_x + v\underset{\sim}{e}_y .$$

We obtain,

$$u = U(1-\zeta) - \frac{\varphi_o}{2}\frac{h^2}{R}\left(\frac{dP}{d\theta}\right)(\zeta-\zeta^2)$$

$$-\frac{\kappa}{6}\frac{h^3}{R^2}\left(\frac{dP}{d\theta}\right)^2(\zeta-\zeta^3) , \quad \zeta = \frac{y}{h} ,$$

where $dx = Rd\theta$ has been used. To compute the pressure gradient, we consider the Reynolds equations for film lubrication written in terms of the pressure and gap size for an inelastic fluid of the linear fluidity type

$$\frac{\partial}{\partial x}\left(h^3\varphi\frac{\partial P}{\partial x}\right) + \frac{\partial}{\partial z}\left(h^3\varphi\frac{\partial P}{\partial z}\right) = 6U\frac{\partial h}{\partial x} ,$$

where (z) is the axial coordinate and (x) is the coordinate on the inner or outer wall. Replacing (x) by the angular coordinate θ and assuming that the pipes are sufficiently long in the axial direction and no pressure gradient acts in that direction, $\partial P/\partial z = 0$, we obtain for the pressure field using the boundary and periodicity conditions,

$$P|_{\theta=0} = P_0 , \quad P|_{\theta=0} = P|_{\theta=2\pi} .$$

$$P = P_0 + \frac{6URe}{\varphi_0 c^2}\frac{(2+\varepsilon\cos\theta)\sin\theta}{(2+\varepsilon^2)(1+\varepsilon\cos\theta)^2}$$

$$+\frac{2\kappa RU^2}{\varphi_0^3 c^3}\frac{(4-\varepsilon^2+3\cos\theta)\sin\theta}{(2+\varepsilon^2)(1+\varepsilon\cos\theta)^2}$$

where P_0 is the pressure at the smallest gap in the cross-section. Using this result in the velocity field gives the following normalized expression for the azimuthal velocity in the eccentric annulus,

$$\frac{u}{U} = 1-\zeta - \frac{3\varepsilon\beta\zeta(1-\zeta)}{\alpha\gamma}\left[1+\frac{2\delta\varepsilon\beta}{\alpha\gamma^2}(1+\zeta)\right] ,$$

$$\alpha = 2+\varepsilon^2 , \quad \beta = 2\cos\theta+3\varepsilon+\varepsilon^2\cos\theta ,$$

$$\gamma = 1+\varepsilon\cos\theta , \quad \delta = \kappa U/\varphi_0^2 c , \quad \varepsilon = e/c , \quad c = R_0 - R .$$

Separation takes place at the outer wall if,

$$\left(\frac{u}{U}\right)_{,\zeta|_{\zeta=1}} = 0 .$$

The locations of the separation and reattachment points on the outer wall may be calculated using this criterion. We obtain,

$$\frac{3\varepsilon\beta}{\alpha\gamma} + \frac{12\delta\varepsilon^2\beta^2}{\alpha^2\gamma^3} = 1 ,$$

which yields a cubic in terms of $\cos\theta$ whose roots determine the separation and reattachment angles θ_s and θ_r, respectively.

EXPERIMENTAL

The experimental setup is sketched in Fig. 2. The hydraulic loop has an inner pipe of diameter 10 cm and a stationary outer pipe of diameter 12 cm. The pipes are long enough, 120 cm each, to neglect end effects. A plexiglass lid was used in

the loop, and in the middle section of the outer pipe there is a plexiglass window for the beam from the flash tube. The inner pipe is belt driven by means of a variable speed motor connected to a tachometer. Available speeds of the inner pipe were up to 100 rpm. The maximum rotational Reynolds number $Re_m = U_m \rho h \varphi$, maximum angular velocity and velocity on the inner rotating surface available in the apparatus are $Re_m = 300$, $\omega_m \sim 10 s^{-1}$ and $U_m = 1 m/s$, respectively. Experiments were performed at $Re \sim 200$ and $\omega \sim 6 s^{-1}$. The eccentricity ratio ε was varied from 0 to 0.5.

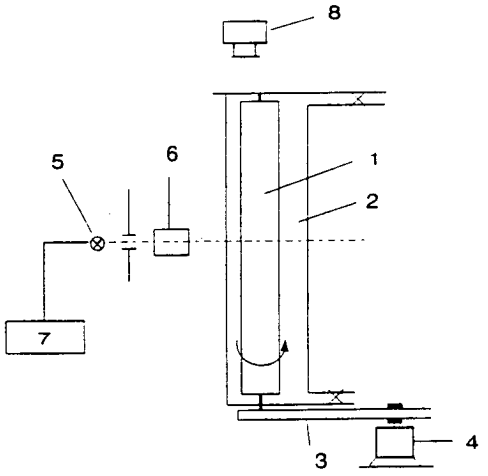

Fig. 2 Experimental setup. 1-rotating inner tube; 2-fixed outer tube; 3-belt drive; 4-variable speed motor; 5-flash tube; 6-convergent lens; 7-electronic stroboscope; 8-camera

For velocity measurements the method of stroboscopic flow visualization was used. In this method, marker particles illuminated by light pulses are photographed and tracked over a finite interval of time. Several images of the same moving particle are recorded on one photographic plate. The particle velocity is computed by means of a picture-processing unit and computer. The Newtonian liquid is a glycerol/water mixture with a viscosity of 0.018 Pa s at 20°C. The non-Newtonian liquid is a shear-thinning spacer fluid used in drilling and cementing operations. The rheological behavior of this polyacrylamide based spacer fluid with several proprietary additives is well described by the linear fluidity model. The particular fluid used in the experiments in this paper contains 0.8% polyacrylamide of molecular weight $2\sim3\times10^6$, with several proprietary additives. This fluid is only very slightly elastic if at all. Normal stress differences are quite small, smaller at the very least by an order of magnitude than those of a 0.1% dilute solution of polyacrylamide of molecular weight 2×10^7.

DISCUSSION AND CONCLUSION

Analytical predictions for one value of the eccentricity ratio $\varepsilon = 0.5$ is shown in Fig. 3 together with experimental data. The azimuthal velocity variation across the gap is parabolic and cubic in the Newtonian and inelastic cases, respectively, when $\varepsilon > 0$. Although the velocity variation is nonlinear, normalized velocity profiles in a given gap are independent of the rotational Reynolds number as they collapse onto a single curve in the range of the available Reynolds numbers in our apparatus. The theory based on the lubrication approximation predicts that azimuthal velocity profiles for the Newtonian fluid ($\delta = 0$) are symmetric about a line through the minimum ($\theta = 180°$) and maximum ($\theta = 0°$) gaps. This is verified by the data for the glycerol/water mixture used in the experiments. Neither the data for the drilling fluid nor the analytical predictions based on the linear fluidity law show any symmetry with respect to the same line joining the centers of the inner and outer walls. The non-Newtonian parameter δ has a large effect on the azimuthal velocity profile at any gap. The theory corroborated by experiments shows that the linear fluidity model fluid has a consistently smaller velocity for all values of δ. The effect of δ becomes more pronounced with increasing eccentricity ratio ε. As ε increases, the azimuthal velocity profiles become increasingly asymmetric. A larger value of δ may be interpreted as a more shear-thinning fluid if other parameters in δ are kept constant. Or equivalently, the inner tube may be rotating faster and/or the radial clearance c may be smaller. Velocity profiles such as those in Fig. 3 may be used to estimate the size of the counter-rotating eddy by tracking the location of the eddy center with varying ε and δ. The eddy grows with growing δ at fixed ε as well as with growing ε at fixed δ as the eddy core comes closer to the

rotating inner wall in either case. We conclude that with this type of fluid the extent of the separated region in the large gap will inevitably increase with an increase either in ε or δ.

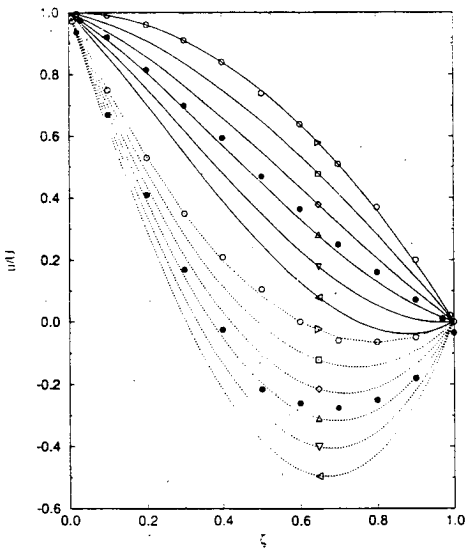

Fig. 3 Velocity profiles in the widest ($\theta = 0°$) and narrowest ($\theta = 180°$) gaps at eccentricity ratio $\varepsilon = 0.5$. Analytical predictions for various values of δ: $\theta = 0°$ (---), $\theta = 180°$ (—); $\delta = 0.0$ ($\triangleright$), $\delta = 0.2$ ($\square$), $\delta = 0.4$ ($\diamond$), $\delta = 0.6$ ($\triangle$), $\delta = 0.8$ ($\triangledown$), $\delta = 1.0$ ($\triangleleft$). Experimental data: ($\circ$) Newtonian liquid, $\delta = 0$; ($\bullet$) shear rate dependent viscosity fluid, $\delta = 0.6$.

These qualitative findings concerning the size of the eddy are further corroborated by the computation of the separation angle θ_s at the outer wall. At fixed ε the separation and the reattachment angles increase with increasing δ, that is, with increasing shear-thinning behavior. θ_s also increases with increasing ε at a fixed value of δ, thus indicating in both cases the tendency of the counter-rotating eddy to grow larger with increasing values of the eccentricity ratio and with increasing non-Newtonian behavior. The lubrication approximation consistently overestimates the separation and reattachment angles in the Newtonian case ($\delta = 0$), thus overestimating the size of the resulting Newtonian eddy. We compute and observe experimentally with drilling fluids consistently smaller velocities as the shear rate dependent behavior becomes stronger which leads to larger eddies.